EUROPEAN ORGANIZATION FOR NUCLEAR RESEARCH

CERN-EP/2001-080
November 6, 2001

Study of the $W^+W^-\gamma$ Process and Limits on Anomalous Quartic Gauge Boson Couplings at LEP

The L3 Collaboration

Abstract

The process $e^+e^- \to W^+W^-\gamma$ is studied using the data collected by the L3 detector at LEP. New results, corresponding to an integrated luminosity of $427.4\,pb^{-1}$ at centre-of-mass energies from 192 GeV to 207 GeV, are presented.

The $W^+W^-\gamma$ cross sections are measured to be in agreement with Standard Model expectations. No hints of anomalous quartic gauge boson couplings are observed. Limits at 95% confidence level are derived using also the process $e^+e^- \to \nu\bar{\nu}\gamma\gamma$.

Submitted to *Phys. Lett. B*

Introduction

The increase of the LEP centre-of-mass energy well above the W boson pair-production threshold opens the possibility of studying the triple boson production process $e^+e^- \to W^+W^-\gamma$. We report on the cross section measurement of this inclusive process where the photon lies inside a defined phase space region.

The three boson final state gives access to quartic gauge boson couplings represented by four-boson interaction vertices as shown in Figure 1a. At the LEP centre-of-mass energies the contribution of four-boson vertex diagrams, predicted by the Standard Model of electroweak interactions [1, 2], are negligible with respect to the other competing diagrams, mainly initial-state radiation. The study of the $W^+W^-\gamma$ process is thus sensitive to anomalous quartic gauge couplings (AQGC) in both the $W^+W^-Z\gamma$ and $W^+W^-\gamma\gamma$ vertices. The presence of AQGC would increase the cross section and modify the photon energy spectrum of the $W^+W^-\gamma$ process. This search is performed within the theoretical framework of References 3 and 4.

The existence of AQGC would also affect the $e^+e^- \to \nu\bar{\nu}\gamma\gamma$ process via the W^+W^- fusion diagram, shown in Figure 1b, containing the $W^+W^-\gamma\gamma$ vertex [5]. The reaction $e^+e^- \to \nu\bar{\nu}\gamma\gamma$ is dominated by initial-state radiation whereas the quartic Standard Model contribution from the W^+W^- fusion is negligible at LEP. Also in this case the presence of AQGC would enhance the production rate, especially for the hard tail of the photon energy distribution and for photons produced at large angles with respect to the beam direction.

The results are based on the high energy data sample collected with the L3 detector [6]. Data at the centre-of-mass energy of $\sqrt{s} = 189$ GeV, corresponding to an integrated luminosity of 176.8 pb^{-1}, were already analysed [7] and are used in the AQGC analysis. In the following, particular emphasis is given to the additional luminosity of 427.4 pb^{-1} recorded at centre-of-mass energies ranging from $\sqrt{s} = 192$ GeV up to 207 GeV.

The results derived on AQGC from the $W^+W^-\gamma$ and $\nu\bar{\nu}\gamma\gamma$ channels are eventually combined.

Studies of triple gauge bosons production and AQGC were recently reported for both the $W^+W^-\gamma$ [8] and $Z\gamma\gamma$ [9] final states.

Monte Carlo Simulation

The dominant contributions to the $W^+W^-\gamma$ final state come from the radiative graphs with photons emitted by the incoming particles (ISR), by the decay products of the W bosons (FSR) or by the W's themselves (WSR).

In this study, the signal is defined as the phase space region of the $e^+e^- \to W^+W^-\gamma$ process where the photon fulfills the following criteria:

- $E_\gamma > 5$ GeV, where E_γ is the energy of the photon,
- $20^\circ < \theta_\gamma < 160^\circ$, where θ_γ is the angle between the photon and the beam axis,
- $\alpha_\gamma > 20^\circ$, where α_γ is the angle between the direction of the photon and that of the closest charged fermion.

These requirements, used to enhance the effect of possible AQGC, largely contribute to avoid infrared and collinear singularities in the calculation of the signal cross section.

In order to study efficiencies, background contaminations and AQGC effects, several Monte Carlo programs are used.

The KORALW [10] generator, which does not include either the quartic coupling diagrams or the WSR, performs initial state multi-photon radiation in the full photon phase space. FSR from charged leptons in the event up to double bremsstrahlung is included using the PHOTOS [11] package. The JETSET [12] Monte Carlo program, which includes photons in the parton shower, is used to model the fragmentation and hadronization process. The KORALW program is used in the analysis for the determination of efficiencies. PYTHIA [13] is used to simulate the background processes: $e^+e^- \to Z/\gamma \to q\bar{q}(\gamma)$, $e^+e^- \to ZZ \to 4f(\gamma)$ and $e^+e^- \to Zee \to ffee(\gamma)$.

The EEWWG [4] program is used to simulate the effect of AQGC. It includes $\mathcal{O}(\alpha)$ calculations for visible photons but is lacking the simulation of photons collinear to the beam pipe and of FSR. The net effect of collinear photons, included by implementing the EXCALIBUR [14] collinear radiator function, is to move the effective centre-of-mass energy towards lower values, reducing the expected signal cross section by about 18%.

Other Monte Carlo programs which include WSR or full $\mathcal{O}(\alpha)$ corrections, such as YFSWW3 [15] and RacoonWW [16], are used to cross check the calculations.

For the simulation of the $e^+e^- \to \nu\bar{\nu}\gamma\gamma$ process in the framework of the Standard Model the KORALZ [17] Monte Carlo generator is used. NUNUGPV [18] is also used to cross check the results, and found to be in agreement with KORALZ. The effects of AQGC are simulated using the EENUNUGGANO program [5]. The missing higher order corrections due to ISR in EENUNUGGANO are also estimated by implementing the EXCALIBUR collinear radiator function.

The response of the L3 detector is modelled with the GEANT [19] detector simulation program which includes the effects of energy loss, multiple scattering and showering in the detector materials and in the beam pipe. Time dependent detector inefficiencies are taken into account in the simulation.

$W^+W^-\gamma$ Event Selection and Cross Section

The selection of $W^+W^-\gamma$ events follows two steps: first semileptonic $W^+W^- \to qqe\nu$ or $qq\mu\nu$, and fully hadronic $W^+W^- \to qqqq$ events are selected [20], then a search for isolated photons is performed.

The photon identification in W^+W^- events is optimized for each four-fermion final state. Photons are identified from energy clusters in the electromagnetic calorimeter not associated with any track in the central detector and with low activity in the nearby region of the hadron calorimeter. The profile of the shower must be consistent with that of an electromagnetic particle. Experimental cuts on photon energy and angles are applied, reflecting the phase space definition of the signal.

Figure 2 shows the distributions of E_γ, θ_γ, and α_γ for the full data set, including the data at $\sqrt{s} = 189$ GeV. Here, α_γ is defined as the angle of the photon with respect to the closest identified lepton or hadronic jet. Good agreement between data and Standard Model expectations is observed. Figure 3 shows the distributions of E_γ for the data collected at $\sqrt{s} = 192 - 202$ GeV and $\sqrt{s} = 205 - 207$ GeV, respectively.

Table 1 summarizes the selection yield. In total 86 $W^+W^-\gamma$ candidate events are selected at $\sqrt{s} = 192 - 207$ GeV. The Standard Model expectation, inside the specified phase space region, is of 87.8 ± 0.8 events.

The quantity ε_{WW}, representing the selection efficiencies for the $W^+W^- \to qql\nu$ and qqqq decay modes, ranges from 70% to 87%. The quantity ε_γ is the photon identification efficiency

inside the selected phase space region. This efficiency takes into account small effects of events migrating from outside the signal region into the selected sample due to the finite detector resolution. Its value ranges from 52% to 80%, the lowest efficiencies being obtained in the fully hadronic sample where the high multiplicity makes the photon identification more difficult. The overall selection efficiency $\varepsilon_{\mathrm{WW}} \times \varepsilon_{\gamma}$ is around 45% for all final states.

The $\mathrm{W^+W^-}\gamma$ cross sections are evaluated channel by channel and then combined according to the Standard Model W boson branching fractions. The data samples at $\sqrt{s} = 192-196$ GeV, $\sqrt{s} = 200-202$ GeV and $\sqrt{s} = 205-207$ GeV are respectively merged. They correspond to the luminosity averaged centre-of-mass energies and to the integrated luminosities listed in Table 1.

The results, including the published value at $\sqrt{s} = 189$ GeV [7], are:

$$\begin{aligned}
\sigma_{\mathrm{WW}\gamma}(188.6\ \mathrm{GeV}) &= 0.29 \pm 0.08 \pm 0.02\ \ \mathrm{pb} \quad (\sigma_{\mathrm{SM}} = 0.233 \pm 0.012\ \ \mathrm{pb}) \\
\sigma_{\mathrm{WW}\gamma}(194.4\ \mathrm{GeV}) &= 0.23 \pm 0.10 \pm 0.02\ \ \mathrm{pb} \quad (\sigma_{\mathrm{SM}} = 0.268 \pm 0.013\ \ \mathrm{pb}) \\
\sigma_{\mathrm{WW}\gamma}(200.2\ \mathrm{GeV}) &= 0.39 \pm 0.12 \pm 0.02\ \ \mathrm{pb} \quad (\sigma_{\mathrm{SM}} = 0.305 \pm 0.015\ \ \mathrm{pb}) \\
\sigma_{\mathrm{WW}\gamma}(206.3\ \mathrm{GeV}) &= 0.33 \pm 0.09 \pm 0.02\ \ \mathrm{pb} \quad (\sigma_{\mathrm{SM}} = 0.323 \pm 0.016\ \ \mathrm{pb}),
\end{aligned}$$

where the first uncertainty is statistical and the second systematic. The measurements are in good agreement with the Standard Model expectations, σ_{SM}, calculated using `EEWWG` and reported with a theoretical uncertainty of 5% [21]. Figure 4 shows these results together with the predicted total $\mathrm{W^+W^-}\gamma$ cross sections as a function of the centre-of-mass energy.

The ratio between the measured cross section σ_{meas} and the theoretical expectations is derived at each centre-of-mass energy. These values are then combined as:

$$R = \frac{\sigma_{\mathrm{meas}}}{\sigma_{\mathrm{SM}}} = 1.09 \pm 0.17 \pm 0.09\ ,$$

where the first uncertainty is statistical and the second systematic.

The systematic uncertainties arising in the inclusive W-pair event selections [20] are propagated to the final measurement and correspond to an uncertainty of 0.008 pb for all the energy points. Additional systematic uncertainties due to the electromagnetic calorimeter resolution and energy scale are found to be negligible. The total systematic uncertainty is dominated by the `JETSET` modelling of photons from meson decays (π^0, η). Its effect has been directly studied on data [7] comparing the photon rate in $\mathrm{e^+e^-} \to \mathrm{Z} \to \mathrm{q\bar{q}}(\gamma)$ events with Monte Carlo simulations. A correction factor of 1.2 ± 0.1 is applied to the rate of photons in the Monte Carlo simulation and its uncertainty is propagated. This uncertainty, fully correlated among the data taking periods, amounts to 6 % of the measured cross section.

Determination of Anomalous Quartic Gauge Couplings

The $\mathrm{e^+e^-} \to \mathrm{W^+W^-}\gamma$ Process

In the framework of References 3 and 4, the Standard Model Lagrangian of electroweak interactions is extended to include dimension-6 operators proportional to the three AQGC: a_0/Λ^2, a_c/Λ^2 and a_n/Λ^2, where Λ^2 represents the energy scale for new physics.

The two parameters a_0/Λ^2 and a_c/Λ^2, which are separately C and P conserving, generate anomalous $\mathrm{W^+W^-}\gamma\gamma$ and $\mathrm{ZZ}\gamma\gamma$ vertices. The term a_n/Λ^2, which is CP violating, gives rise to an anomalous contribution to the $\mathrm{W^+W^-Z}\gamma$ vertex. Indirect limits on a_0/Λ^2 and a_c/Λ^2 were derived [22], but only the study of $\mathrm{W^+W^-}\gamma$ events allows for a direct measurement of the

anomalous coupling a_n/Λ^2. These couplings would manifest themselves by modifying the energy spectrum of the photons and the total cross section as shown in Figures 3 and 4, respectively. The effect increases with increasing centre-of-mass energy. These predictions are obtained by reweighting the KORALW Monte Carlo events by the ratio of the differential distributions as calculated by the EEWWG and KORALW programs [7].

The derivation of AQGC is performed by fitting both the shape and the normalization of the photon energy spectrum in the range from 5 GeV to 35 GeV. Each of the AQGC is varied in turn fixing the other two to zero.

The combination of all data, including the results at $\sqrt{s} = 189$ GeV [7], gives:

$$\begin{aligned} a_0/\Lambda^2 &= 0.000 \pm 0.010 \text{ GeV}^{-2} \\ a_c/\Lambda^2 &= -0.013 \pm 0.023 \text{ GeV}^{-2} \\ a_n/\Lambda^2 &= -0.002 \pm 0.076 \text{ GeV}^{-2} \end{aligned}$$

where systematic uncertainties are included.

At the 95% confidence level, the AQGC are constrained to:

$$\begin{aligned} -0.017 \text{ GeV}^{-2} &< a_0/\Lambda^2 < 0.017 \text{ GeV}^{-2} \\ -0.052 \text{ GeV}^{-2} &< a_c/\Lambda^2 < 0.026 \text{ GeV}^{-2} \\ -0.14 \text{ GeV}^{-2} &< a_n/\Lambda^2 < 0.13 \text{ GeV}^{-2}. \end{aligned}$$

All these results are in agreement with the Standard Model expectation. The sign of the a_0 and a_c AQGC, obtained with the EEWWG reweighting, is reversed according to the discussions in References 23 and 24.

The $e^+e^- \to \nu\bar{\nu}\gamma\gamma$ Process

The sensitivity of the $e^+e^- \to \nu\bar{\nu}\gamma\gamma$ process to the a_0/Λ^2 and a_c/Λ^2 AQGC, through the diagrams shown in Figure 1b, is also exploited. Events with an acoplanar multi-photon signature are selected [25]. In this letter we report on results from data at $\sqrt{s} = 192 - 207$ GeV.

Figure 5 shows the two-photon recoil mass, $M_{\rm rec}$, distribution, with the predicted AQGC signal for a non-zero anomalous coupling a_0/Λ^2. The number of selected events in the Z peak region, defined as 75 GeV $< M_{\rm rec} <$ 110 GeV, is 43 in agreement with the Standard Model expectation of 47.6 ± 0.7.

The AQGC signal prediction is reliable only for recoil masses lower than the mass of the Z boson as the interference with the Standard Model processes is not included in the calculation. Requiring $M_{\rm rec} < 75$ GeV, no event is retained by the selection in agreement with the Standard Model expectation of 0.35 ± 0.05 events.

A reweighting technique based on the full matrix elements as calculated by the EENUNUGGANO Monte Carlo, is used to derive the AQGC values. Including the results at $\sqrt{s} = 183$ GeV and $\sqrt{s} = 189$ GeV [7], the 95% confidence level upper limits are:

$$\begin{aligned} -0.031 \text{ GeV}^{-2} &< a_0/\Lambda^2 < 0.031 \text{ GeV}^{-2} \\ -0.090 \text{ GeV}^{-2} &< a_c/\Lambda^2 < 0.090 \text{ GeV}^{-2}, \end{aligned}$$

where only one parameter is varied at a time.

The dominant systematic uncertainty comes from the theoretical uncertainty of 5% [21] in the calculation of anomalous cross sections.

Combined Results

The results obtained from the $W^+W^-\gamma$ and $\nu\bar{\nu}\gamma\gamma$ processes are combined. No evidence of AQGC is found and 95% confidence level limits are obtained separately on each coupling as:

$$\begin{aligned} -0.015\ \text{GeV}^{-2} &< a_0/\Lambda^2 < 0.015\ \text{GeV}^{-2} \\ -0.048\ \text{GeV}^{-2} &< a_c/\Lambda^2 < 0.026\ \text{GeV}^{-2} \\ -0.14\ \ \text{GeV}^{-2} &< a_n/\Lambda^2 < 0.13\ \ \text{GeV}^{-2}. \end{aligned}$$

Appendix

The results on the $e^+e^- \to W^+W^-\gamma$ cross sections are also expressed for a different phase space region defined by:

- $E_\gamma > 5$ GeV,
- $|\cos(\theta_\gamma)| < 0.95$,
- $\cos(\alpha_\gamma) < 0.90$,
- $M_{ff'} = M_W \pm 2\Gamma_W$, where $M_{ff'}$ are the two fermion-pair invariant masses.

The results read:

$$\begin{aligned} \sigma_{WW\gamma}(188.6\ \text{GeV}) &= 0.20 \pm 0.09 \pm 0.01\ \ \text{pb} \quad (\sigma_{SM} = 0.190 \pm 0.010\ \ \text{pb}) \\ \sigma_{WW\gamma}(194.4\ \text{GeV}) &= 0.17 \pm 0.10 \pm 0.01\ \ \text{pb} \quad (\sigma_{SM} = 0.219 \pm 0.011\ \ \text{pb}) \\ \sigma_{WW\gamma}(200.2\ \text{GeV}) &= 0.43 \pm 0.13 \pm 0.02\ \ \text{pb} \quad (\sigma_{SM} = 0.242 \pm 0.012\ \ \text{pb}) \\ \sigma_{WW\gamma}(206.3\ \text{GeV}) &= 0.13 \pm 0.08 \pm 0.01\ \ \text{pb} \quad (\sigma_{SM} = 0.259 \pm 0.013\ \ \text{pb}), \end{aligned}$$

where the first uncertainty is statistical, the second systematic and the values in parentheses indicate the Standard Model predictions.

Author List

The L3 Collaboration:

P.Achard,[20] O.Adriani,[17] M.Aguilar-Benitez,[24] J.Alcaraz,[24,18] G.Alemanni,[22] J.Allaby,[18] A.Aloisio,[28] M.G.Alviggi,[28] H.Anderhub,[47] V.P.Andreev,[6,33] F.Anselmo,[9] A.Arefiev,[27] T.Azemoon,[3] T.Aziz,[10,18] P.Bagnaia,[38] A.Bajo,[24] G.Baksay,[16] L.Baksay,[25] S.V.Baldew,[2] S.Banerjee,[10] Sw.Banerjee,[4] A.Barczyk,[47,45] R.Barillère,[18] P.Bartalini,[22] M.Basile,[9] N.Batalova,[44] R.Battiston,[32] A.Bay,[22] F.Becattini,[17] U.Becker,[14] F.Behner,[47] L.Bellucci,[17] R.Berbeco,[3] J.Berdugo,[24] P.Berges,[14] B.Bertucci,[32] B.L.Betev,[47] M.Biasini,[32] M.Biglietti,[28] A.Biland,[47] J.J.Blaising,[4] S.C.Blyth,[34] G.J.Bobbink,[2] A.Böhm,[1] L.Boldizsar,[13] B.Borgia,[38] S.Bottai,[17] D.Bourilkov,[47] M.Bourquin,[20] S.Braccini,[20] J.G.Branson,[40] F.Brochu,[4] A.Buijs,[43] J.D.Burger,[14] W.J.Burger,[32] X.D.Cai,[14] M.Capell,[14] G.Cara Romeo,[9] G.Carlino,[28] A.Cartacci,[17] J.Casaus,[24] F.Cavallari,[38] N.Cavallo,[35] C.Cecchi,[32] M.Cerrada,[24] M.Chamizo,[20] Y.H.Chang,[49] M.Chemarin,[23] A.Chen,[49] G.Chen,[7] G.M.Chen,[7] H.F.Chen,[21] H.S.Chen,[7] G.Chiefari,[28] L.Cifarelli,[39] F.Cindolo,[9] I.Clare,[14] R.Clare,[37] G.Coignet,[4] N.Colino,[24] S.Costantini,[38] B.de la Cruz,[24] S.Cucciarelli,[32] J.A.van Dalen,[30] R.de Asmundis,[28] P.Déglon,[20] J.Debreczeni,[13] A.Degré,[4] K.Deiters,[45] D.della Volpe,[28] E.Delmeire,[20] P.Denes,[36] F.DeNotaristefani,[38] A.De Salvo,[47] M.Diemoz,[38] M.Dierckxsens,[2] D.van Dierendonck,[2] C.Dionisi,[38] M.Dittmar,[47,18] A.Doria,[28] M.T.Dova,[11,♯] D.Duchesneau,[4] P.Duinker,[2] B.Echenard,[20] A.Eline,[18] H.El Mamouni,[23] A.Engler,[34] F.J.Eppling,[14] A.Ewers,[1] P.Extermann,[20] M.A.Falagan,[24] S.Falciano,[38] A.Favara,[31] J.Fay,[23] O.Fedin,[33] M.Felcini,[47] T.Ferguson,[34] H.Fesefeldt,[1] E.Fiandrini,[32] J.H.Field,[20] F.Filthaut,[30] P.H.Fisher,[14] W.Fisher,[36] I.Fisk,[40] G.Forconi,[14] K.Freudenreich,[47] C.Furetta,[26] Yu.Galaktionov,[27,14] S.N.Ganguli,[10] P.Garcia-Abia,[5,18] M.Gataullin,[31] S.Gentile,[38] S.Giagu,[38] Z.F.Gong,[21] G.Grenier,[23] O.Grimm,[47] M.W.Gruenewald,[8,1] M.Guida,[39] R.van Gulik,[2] V.K.Gupta,[36] A.Gurtu,[10] L.J.Gutay,[44] D.Haas,[5] D.Hatzifotiadou,[9] T.Hebbeker,[8,1] A.Hervé,[18] J.Hirschfelder,[34] H.Hofer,[47] M.Hohlmann,[25] G.Holzner,[47] S.R.Hou,[49] Y.Hu,[30] B.N.Jin,[7] L.W.Jones,[3] P.de Jong,[2] I.Josa-Mutuberría,[24] D.Käfer,[1] M.Kaur,[15] M.N.Kienzle-Focacci,[20] J.K.Kim,[42] J.Kirkby,[18] W.Kittel,[30] A.Klimentov,[14,27] A.C.König,[30] M.Kopal,[44] V.Koutsenko,[14,27] M.Kräber,[47] R.W.Kraemer,[34] W.Krenz,[1] A.Krüger,[46] A.Kunin,[14] P.Ladron de Guevara,[24] I.Laktineh,[23] G.Landi,[17] M.Lebeau,[18] A.Lebedev,[14] P.Lebrun,[23] P.Lecomte,[47] P.Lecoq,[18] P.Le Coultre,[47] J.M.Le Goff,[18] R.Leiste,[46] P.Levtchenko,[33] C.Li,[21] S.Likhoded,[46] C.H.Lin,[49] W.T.Lin,[49] F.L.Linde,[2] L.Lista,[28] Z.A.Liu,[7] W.Lohmann,[46] E.Longo,[38] Y.S.Lu,[7] K.Lübelsmeyer,[1] C.Luci,[38] L.Luminari,[38] W.Lustermann,[47] W.G.Ma,[21] L.Malgeri,[20] A.Malinin,[27] C.Maña,[24] D.Mangeol,[30] J.Mans,[36] J.P.Martin,[23] F.Marzano,[38] K.Mazumdar,[10] R.R.McNeil,[6] S.Mele,[18,28] L.Merola,[28] M.Meschini,[17] W.J.Metzger,[30] A.Mihul,[12] H.Milcent,[18] G.Mirabelli,[38] J.Mnich,[1] G.B.Mohanty,[10] G.S.Muanza,[23] A.J.M.Muijs,[2] B.Musicar,[40] M.Musy,[38] S.Nagy,[16] S.Natale,[20] M.Napolitano,[28] F.Nessi-Tedaldi,[47] H.Newman,[31] T.Niessen,[1] A.Nisati,[38] H.Nowak,[46] R.Ofierzynski,[47] G.Organtini,[38] C.Palomares,[18] D.Pandoulas,[1] P.Paolucci,[28] R.Paramatti,[38] G.Passaleva,[17] S.Patricelli,[28] T.Paul,[11] M.Pauluzzi,[32] C.Paus,[14] F.Pauss,[47] M.Pedace,[38] S.Pensotti,[26] D.Perret-Gallix,[4] B.Petersen,[30] D.Piccolo,[28] F.Pierella,[9] M.Pioppi,[32] P.A.Piroué,[36] E.Pistolesi,[26] V.Plyaskin,[27] M.Pohl,[20] V.Pojidaev,[17] J.Pothier,[18] D.O.Prokofiev,[44] D.Prokofiev,[33] J.Quartieri,[39] G.Rahal-Callot,[47] M.A.Rahaman,[10] P.Raics,[16] N.Raja,[10] R.Ramelli,[47] P.G.Rancoita,[26] R.Ranieri,[17] A.Raspereza,[46] P.Razis,[29] D.Ren,[47] M.Rescigno,[38] S.Reucroft,[11] S.Riemann,[46] K.Riles,[3] B.P.Roe,[3] L.Romero,[24] A.Rosca,[8] S.Rosier-Lees,[4] S.Roth,[1] C.Rosenbleck,[1] B.Roux,[30] J.A.Rubio,[18] G.Ruggiero,[17] H.Rykaczewski,[47] A.Sakharov,[47] S.Saremi,[6] S.Sarkar,[38] J.Salicio,[18] E.Sanchez,[24] M.P.Sanders,[30] C.Schäfer,[18] V.Schegelsky,[33] S.Schmidt-Kaerst,[1] D.Schmitz,[1] H.Schopper,[48] D.J.Schotanus,[30] G.Schwering,[1] C.Sciacca,[28] L.Servoli,[32] S.Shevchenko,[31] N.Shivarov,[41] V.Shoutko,[14] E.Shumilov,[27] A.Shvorob,[31] T.Siedenburg,[1] D.Son,[42] P.Spillantini,[17] M.Steuer,[14] D.P.Stickland,[36] B.Stoyanov,[41] A.Straessner,[18] K.Sudhakar,[10] G.Sultanov,[41] L.Z.Sun,[21] S.Sushkov,[8] H.Suter,[47] J.D.Swain,[11] Z.Szillasi,[25,¶] X.W.Tang,[7] P.Tarjan,[16] L.Tauscher,[5] L.Taylor,[11] B.Tellili,[23] D.Teyssier,[23] C.Timmermans,[30] Samuel C.C.Ting,[14] S.M.Ting,[14] S.C.Tonwar,[10,18] J.Tóth,[13] C.Tully,[36] K.L.Tung,[7] J.Ulbricht,[47] E.Valente,[38] R.T.Van de Walle,[30] V.Veszpremi,[25] G.Vesztergombi,[13] I.Vetlitsky,[27] D.Vicinanza,[39] P.Violini,[38] G.Viertel,[47] S.Villa,[37] M.Vivargent,[4] S.Vlachos,[5] I.Vodopianov,[33] H.Vogel,[34] H.Vogt,[46] I.Vorobiev,[3427] A.A.Vorobyov,[33] M.Wadhwa,[5] W.Wallraff,[1] X.L.Wang,[21] Z.M.Wang,[21] M.Weber,[1] P.Wienemann,[1] H.Wilkens,[30] S.Wynhoff,[36] L.Xia,[31] Z.Z.Xu,[21] J.Yamamoto,[3] B.Z.Yang,[21] C.G.Yang,[7] H.J.Yang,[3] M.Yang,[7] S.C.Yeh,[50] An.Zalite,[33] Yu.Zalite,[33] Z.P.Zhang,[21] J.Zhao,[21] G.Y.Zhu,[7] R.Y.Zhu,[31] H.L.Zhuang,[7] A.Zichichi,[9,18,19] G.Zilizi,[25,¶] B.Zimmermann,[47] M.Zöller.[1]

1 I. Physikalisches Institut, RWTH, D-52056 Aachen, FRG[§]
III. Physikalisches Institut, RWTH, D-52056 Aachen, FRG[§]
2 National Institute for High Energy Physics, NIKHEF, and University of Amsterdam, NL-1009 DB Amsterdam, The Netherlands
3 University of Michigan, Ann Arbor, MI 48109, USA
4 Laboratoire d'Annecy-le-Vieux de Physique des Particules, LAPP,IN2P3-CNRS, BP 110, F-74941 Annecy-le-Vieux CEDEX, France
5 Institute of Physics, University of Basel, CH-4056 Basel, Switzerland
6 Louisiana State University, Baton Rouge, LA 70803, USA
7 Institute of High Energy Physics, IHEP, 100039 Beijing, China[△]
8 Humboldt University, D-10099 Berlin, FRG[§]
9 University of Bologna and INFN-Sezione di Bologna, I-40126 Bologna, Italy
10 Tata Institute of Fundamental Research, Mumbai (Bombay) 400 005, India
11 Northeastern University, Boston, MA 02115, USA
12 Institute of Atomic Physics and University of Bucharest, R-76900 Bucharest, Romania
13 Central Research Institute for Physics of the Hungarian Academy of Sciences, H-1525 Budapest 114, Hungary[‡]
14 Massachusetts Institute of Technology, Cambridge, MA 02139, USA
15 Panjab University, Chandigarh 160 014, India.
16 KLTE-ATOMKI, H-4010 Debrecen, Hungary[¶]
17 INFN Sezione di Firenze and University of Florence, I-50125 Florence, Italy
18 European Laboratory for Particle Physics, CERN, CH-1211 Geneva 23, Switzerland
19 World Laboratory, FBLJA Project, CH-1211 Geneva 23, Switzerland
20 University of Geneva, CH-1211 Geneva 4, Switzerland
21 Chinese University of Science and Technology, USTC, Hefei, Anhui 230 029, China[△]
22 University of Lausanne, CH-1015 Lausanne, Switzerland
23 Institut de Physique Nucléaire de Lyon, IN2P3-CNRS,Université Claude Bernard, F-69622 Villeurbanne, France
24 Centro de Investigaciones Energéticas, Medioambientales y Tecnológicas, CIEMAT, E-28040 Madrid, Spain[♭]
25 Florida Institute of Technology, Melbourne, FL 32901, USA
26 INFN-Sezione di Milano, I-20133 Milan, Italy
27 Institute of Theoretical and Experimental Physics, ITEP, Moscow, Russia
28 INFN-Sezione di Napoli and University of Naples, I-80125 Naples, Italy
29 Department of Physics, University of Cyprus, Nicosia, Cyprus
30 University of Nijmegen and NIKHEF, NL-6525 ED Nijmegen, The Netherlands
31 California Institute of Technology, Pasadena, CA 91125, USA
32 INFN-Sezione di Perugia and Università Degli Studi di Perugia, I-06100 Perugia, Italy
33 Nuclear Physics Institute, St. Petersburg, Russia
34 Carnegie Mellon University, Pittsburgh, PA 15213, USA
35 INFN-Sezione di Napoli and University of Potenza, I-85100 Potenza, Italy
36 Princeton University, Princeton, NJ 08544, USA
37 University of Californa, Riverside, CA 92521, USA
38 INFN-Sezione di Roma and University of Rome, "La Sapienza", I-00185 Rome, Italy
39 University and INFN, Salerno, I-84100 Salerno, Italy
40 University of California, San Diego, CA 92093, USA
41 Bulgarian Academy of Sciences, Central Lab. of Mechatronics and Instrumentation, BU-1113 Sofia, Bulgaria
42 The Center for High Energy Physics, Kyungpook National University, 702-701 Taegu, Republic of Korea
43 Utrecht University and NIKHEF, NL-3584 CB Utrecht, The Netherlands
44 Purdue University, West Lafayette, IN 47907, USA
45 Paul Scherrer Institut, PSI, CH-5232 Villigen, Switzerland
46 DESY, D-15738 Zeuthen, FRG
47 Eidgenössische Technische Hochschule, ETH Zürich, CH-8093 Zürich, Switzerland
48 University of Hamburg, D-22761 Hamburg, FRG
49 National Central University, Chung-Li, Taiwan, China
50 Department of Physics, National Tsing Hua University, Taiwan, China
§ Supported by the German Bundesministerium für Bildung, Wissenschaft, Forschung und Technologie
‡ Supported by the Hungarian OTKA fund under contract numbers T019181, F023259 and T024011.
¶ Also supported by the Hungarian OTKA fund under contract number T026178.
♭ Supported also by the Comisión Interministerial de Ciencia y Tecnología.
♯ Also supported by CONICET and Universidad Nacional de La Plata, CC 67, 1900 La Plata, Argentina.
△ Supported by the National Natural Science Foundation of China.

References

[1] S. L. Glashow, Nucl. Phys. **22** (1961) 579; S. Weinberg, Phys. Rev. Lett. **19** (1967) 1264; A. Salam, in *Elementary Particle Theory*, ed. N. Svartholm, Stockholm, Almquist and Wiksell (1968), 367

[2] M. Veltman, Nucl. Phys. **B7** (1968) 637; G.M. 't Hooft, Nucl. Phys. **B35** (1971) 167; G.M. 't Hooft and M. Veltman, Nucl. Phys. **B44** (1972) 189; Nucl. Phys. **B50** (1972) 318

[3] G. Bélanger and F. Boudjema, Nucl. Phys. **B288** (1992) 201

[4] J.W. Stirling and A. Werthenbach, Eur. Phys. J. **C14** (2000) 103

[5] J.W. Stirling and A. Werthenbach, Phys. Lett. **B466** (1999) 369

[6] L3 Collab., B. Adeva *et al.*, Nucl. Instr. Meth. **A289** (1990) 35; J. A. Bakken *et al.*, Nucl. Instr. Meth. **A275** (1989) 81; O. Adriani *et al.*, Nucl. Instr. Meth. **A302** (1991) 53; B. Adeva *et al.*, Nucl. Instr. Meth. **A323** (1992) 109; K. Deiters *et al.*, Nucl. Instr. Meth. **A323** (1992) 162; M. Chemarin *et al.*, Nucl. Instr. Meth. **A349** (1994) 345; M. Acciarri *et al.*, Nucl. Instr. Meth. **A351** (1994) 300; G. Basti *et al.*, Nucl. Instr. Meth. **A374** (1996) 293; A. Adam *et al.*, Nucl. Instr. Meth. **A383** (1996) 342

[7] L3 Collab., M. Acciarri *et al.*, Phys. Lett. **B490** (2000) 187

[8] Opal Collab., G. Abbiendi *et al.*, Phys. Lett. **B471** (1999) 293

[9] L3 Collab., M. Acciarri *et al.*, Phys. Lett. **B478** (2000) 34; Phys. Lett. **B505** (2001) 47

[10] KORALW version 1.33 is used,
S. Jadach *et al.*, Comp. Phys. Comm. **94** (1996) 216; S. Jadach *et al.*, Phys. Lett. **B372** (1996) 289

[11] E. Barberio, B. van Eijk and Z. Was, Comp. Phys. Comm. **79** (1994) 291

[12] JETSET version 7.409 is used,
T. Sjöstrand and H. U. Bengtsson, Comp. Phys. Comm. **46** (1987) 43

[13] PYTHIA version 5.722 is used,
T. Sjöstrand, Comp. Phys. Comm. **82** (1994) 74

[14] F.A. Berends, R. Pittau and R. Kleiss, Comp. Phys. Comm. **85** (1995) 437

[15] YFSWW3 version 1.14 is used,
S. Jadach *et al.*, Phys. Rev. **D54** (1996) 5434; Phys. Lett. **B417** (1998) 326; Phys. Rev. **D61** (2000) 113010; preprint hep-ph/0007012 (2000)

[16] A. Denner *et al.*, Phys. Lett. **B475** (2000) 127; Nucl. Phys. **B587** (2000) 67.

[17] KORALZ version 4.03 is used,
S. Jadach *et al.*, Comp. Phys. Comm. **79** (1994) 503

[18] G. Montagna *et al.*, Nucl. Phys. **B541** (1999) 31

[19] GEANT Version 3.15 is used,
R. Brun *et al.*, "GEANT 3", preprint CERN DD/EE/84-1 (1984), revised 1987.
The GHEISHA program (H. Fesefeldt, RWTH Aachen Report PITHA 85/02 (1985)) is used to simulate hadronic interactions

[20] L3 Collab., M. Acciarri *et al.*, Phys. Lett. **B496** (2000) 19

[21] J.W. Stirling and A. Werthenbach, private communication

[22] O.J.P. Eboli and M.C. Gonzales–Garcia, Phys. Lett. **B411** (1994) 381

[23] A. Denner *et al.*, Eur. Phys. J. **C20** (2001) 201

[24] G. Montagna *et al.*, Phys. Lett. **B515** (2001) 197

[25] L3 Collab., M. Acciarri *et al.*, Phys. Lett. **B444** (1998) 503; Phys. Lett. **B470** (1999) 268.

$\langle\sqrt{s}\rangle$	Channel	N_{data}	$\varepsilon_{\mathrm{WW}}$	ε_γ	N_{TOT}^{exp}	N_{Bkgr}^{exp}
194.4 GeV	qqe$\nu\gamma$	4	0.748 ± 0.007	0.613 ± 0.023	3.76 ± 0.14	1.41 ± 0.09
(113.4 pb^{-1})	qq$\mu\nu\gamma$	6	0.731 ± 0.007	0.728 ± 0.026	4.52 ± 0.15	1.68 ± 0.09
	qqqqγ	9	0.865 ± 0.004	0.537 ± 0.013	12.89 ± 0.34	5.22 ± 0.28
200.2 GeV	qqe$\nu\gamma$	5	0.726 ± 0.007	0.631 ± 0.023	4.28 ± 0.14	1.47 ± 0.08
(119.8 pb^{-1})	qq$\mu\nu\gamma$	4	0.712 ± 0.007	0.744 ± 0.025	5.50 ± 0.16	2.07 ± 0.10
	qqqqγ	18	0.836 ± 0.004	0.521 ± 0.012	13.71 ± 0.29	5.31 ± 0.28
206.3 GeV	qqe$\nu\gamma$	7	0.700 ± 0.005	0.626 ± 0.024	6.58 ± 0.22	2.21 ± 0.13
(194.2 pb^{-1})	qq$\mu\nu\gamma$	4	0.714 ± 0.005	0.787 ± 0.026	9.54 ± 0.26	3.48 ± 0.16
	qqqqγ	29	0.823 ± 0.005	0.540 ± 0.011	26.97 ± 0.50	12.11 ± 0.39

Table 1: Number of observed events, N_{data}, $\mathrm{W^+W^-}$ and $\mathrm{W^+W^-}\gamma$ selection efficiencies, $\varepsilon_{\mathrm{WW}}$ and ε_γ, expected total number of events, N_{TOT}^{exp}, and background estimates, N_{Bkgr}^{exp}, for the various decay channels according to the Standard Model prediction. The background estimates include FSR and misidentified photons. All uncertainties come from Monte Carlo statistics. The average centre-of-mass energies, $\langle\sqrt{s}\rangle$, and the integrated luminosity of the three subsamples are also listed.

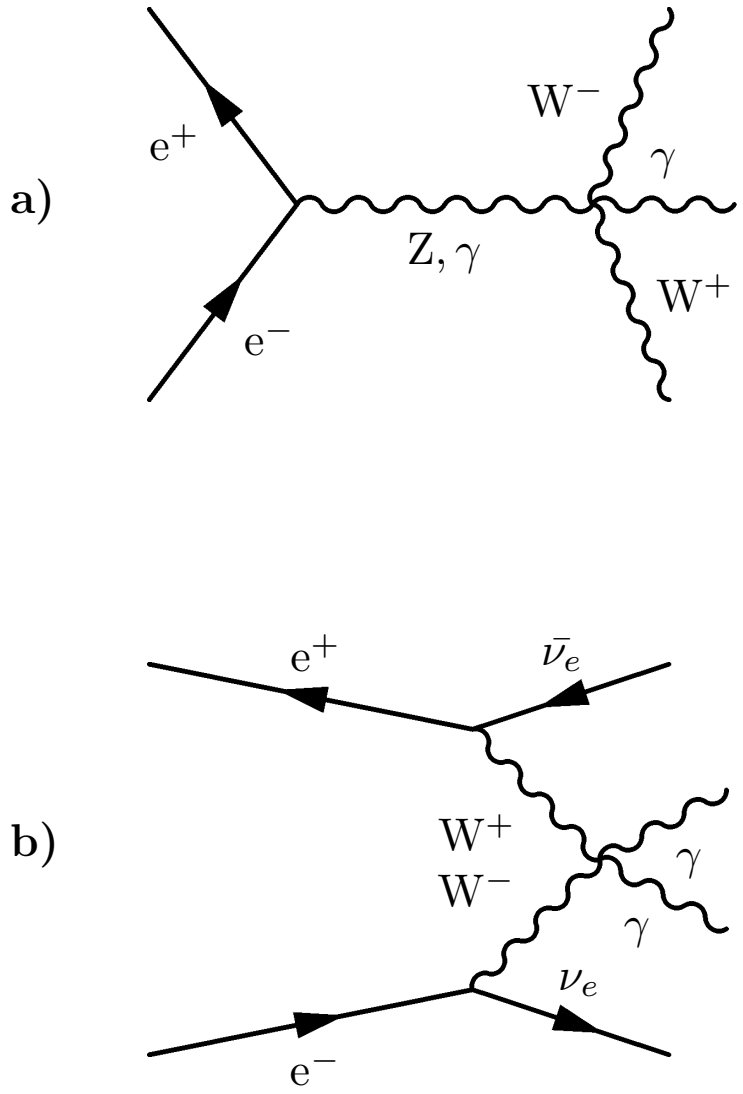

Figure 1: Feynman diagrams containing four-boson vertices leading to the a) $W^+W^-\gamma$ and b) $\nu\bar{\nu}\gamma\gamma$ final states.

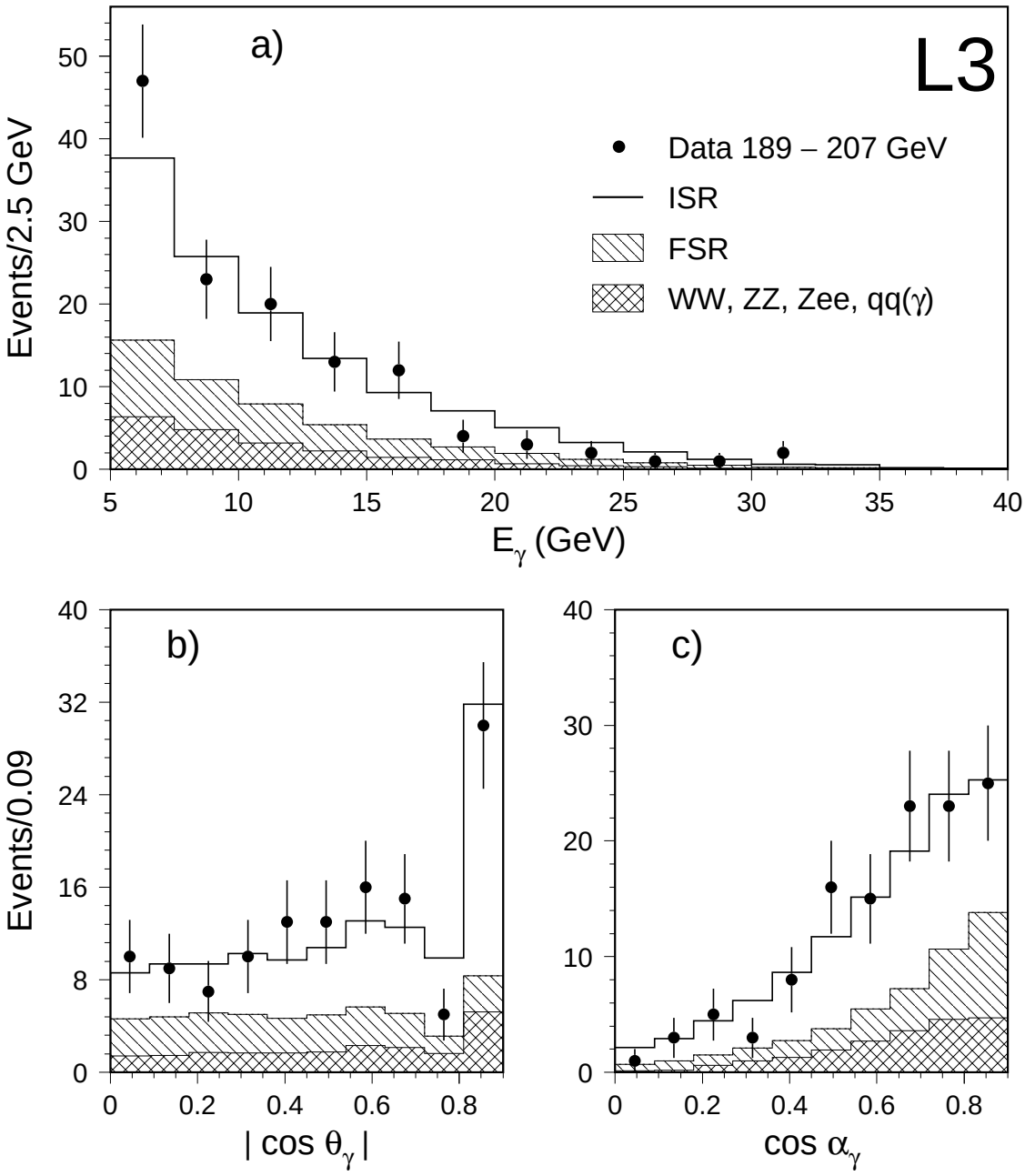

Figure 2: Distributions at the centre-of-mass energies $\sqrt{s} = 189 - 207$ GeV of a) the photon energy, b) the cosine of the angle of the photon to the beam axis and c) the cosine of the angle of the photon to the closest charged lepton or jet.

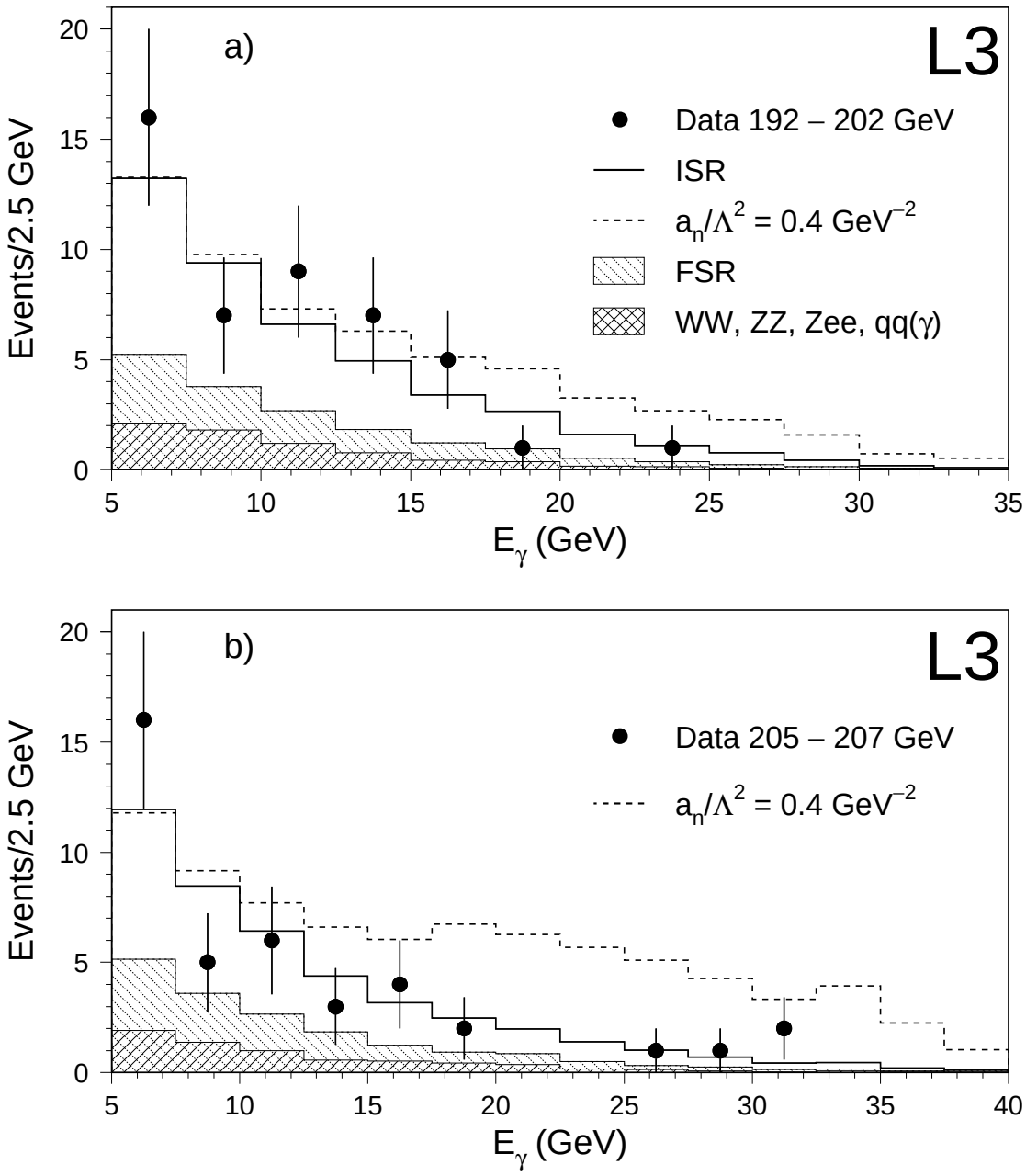

Figure 3: Distributions of the photon energy for the semileptonic qqeν, qq$\mu\nu$ and fully hadronic $W^+W^-\gamma$ decay modes corresponding to the data collected at a) $\sqrt{s} = 192 - 202$ GeV and b) $\sqrt{s} = 205 - 207$ GeV. The cross-hatched area is the background component from WW, ZZ, Zee, and $q\bar{q}(\gamma)$ events. The FSR distribution includes the contribution of photons radiated off the charged fermions and photons originating from isolated meson decays. Distributions corresponding to non-zero values of the anomalous coupling a_n/Λ^2 are shown as dashed lines.

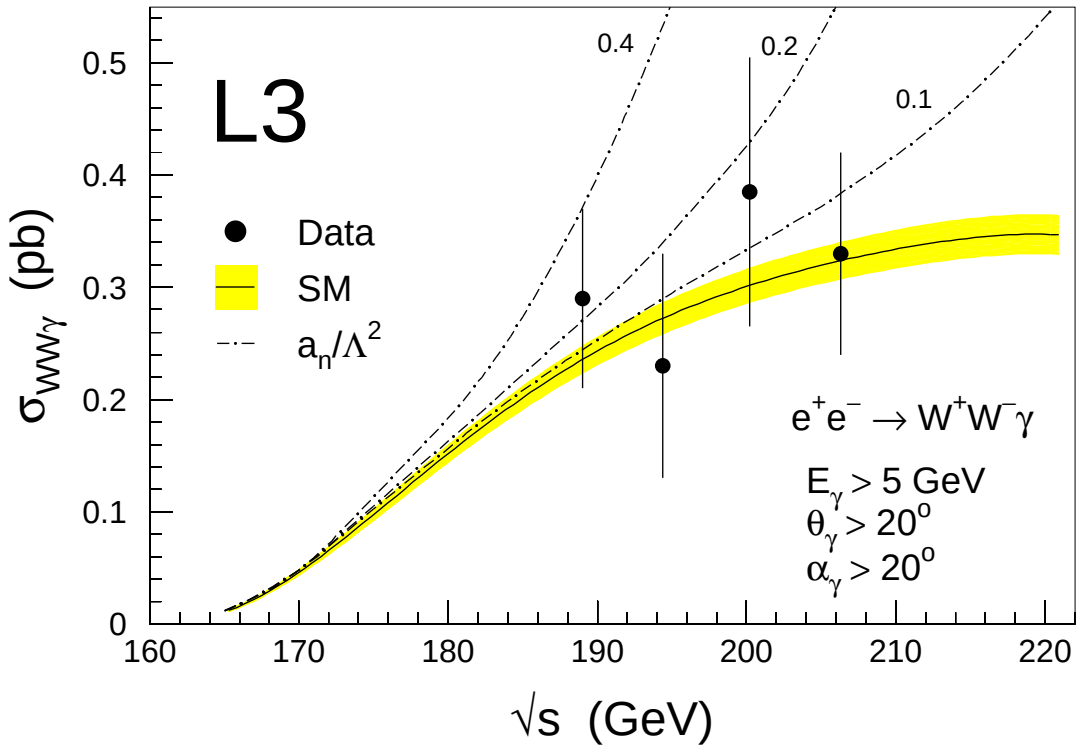

Figure 4: Measured cross section for the process $e^+e^- \to W^+W^-\gamma$ compared to the Standard Model cross section as a function of the centre-of-mass energy, as predicted by the `EEWWG` Monte Carlo within phase-space requirements. The shaded band corresponds to a theoretical uncertainty of $\pm 5\%$. The three dash-dotted lines correspond to the cross section for the indicated values of the anomalous coupling a_n/Λ^2 (in GeV^{-2} units).

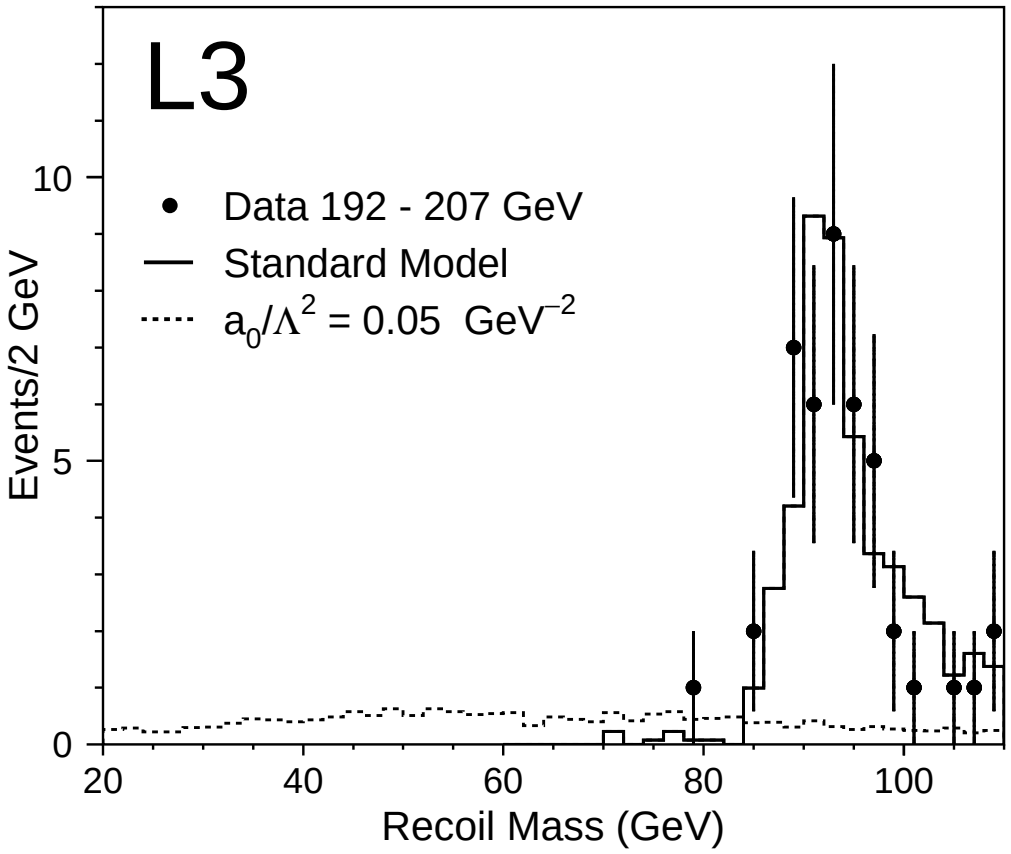

Figure 5: Recoil mass spectrum of the acoplanar photon pair events selected at $\sqrt{s} = 192 - 207$ GeV.